Program Digest, 2019 IEEE International Ultrasonics Symposium (IUS)
Glasgow, Scotland, October 6-9, 2019

Construction of adaptively regularized parametric maps for quantitative ultrasound imaging

François Destrempes
Laboratory of Biorheology and Medical Ultrasonics, University of Montreal Hospital Research Center (CRCHUM),
Montréal, Canada

Marc Gesnik
Laboratory of Biorheology and Medical Ultrasonics, University of Montreal Hospital Research Center (CRCHUM),
Montréal, Canada

Guy Cloutier
Laboratory of Biorheology and Medical Ultrasonics, University of Montreal Hospital Research Center (CRCHUM,)
Montréal, Canada

and
Department of Radiology, Radio-Oncology and Nuclear Medicine, and Institute of Biomedical Engineering, University of Montreal,
Montréal, Canada
guy.cloutier@umontreal.ca

Abstract*—In the field of quantitative ultrasound (QUS), constructing semantic parametric maps based on local attenuation coefficient slope (ACS) or backscatter coefficient (BSC) modeling remains a challenge. These maps may be useful for detecting lesions or anatomical objects, or for characterizing anomalies within organs. The objective was to propose a methodology for constructing regularized parametric maps in the case of linear fitting models. The proposed method was tested on: *i*) the spectral Gaussian fit (SGF) BSC model, comprising the acoustical concentration and effective scatterer size; and *ii*) the spectral log-difference (SLD) model, yielding the local ACS. Regularization was formulated as generalized LASSO, upon setting a locally constant trend constraint on regression coefficients, with variable Lagrangian multiplier (LM). The latter was set with a variant of the Bayesian Information Criterion (BIC): the LM was maximized as to yield a BIC no worse than that of the maximum likelihood. Phantoms were made with agar and graphite powder (g.p.). Acquisitions were performed with a Verasonics Vantage 256 (Redmond, WA) scanner using an ATL L7-4 probe (Philips, Bothell, WA) driven at 5 MHz. Using 21 angles (-5^o to 5^o) compounding, 100 frames were acquired. Beamformed radiofrequency data were averaged over all frames. Power spectra were averaged over 15 scan lines, each spanning 10 pulse lengths, on overlapping windows. Acquisitions with same settings were made on a reference phantom (117GU-101 CIRS, Norfolk, VA). Ground truth ACS values were estimated with a planar reflection method yielding (in dB/cm/MHz): #1) 0.56 ± 0.06 (4.5% g.p.); and #2) 1.27 ± 0.09 (12% g.p.). *i*) *SGF results:* On phantoms with an inclusion (*N* = 4, #2 surrounded by #1), the contrast-to-noise ratio on difference in acoustic concentration (log-scale) was 2.7 ± 0.22 (no units) with regularization, and 0.97 ± 0.13 without it. *ii*) *SLD results:* On phantoms with side-by-side media (*N* = 3), biases were: #1) -0.11 ± 0.04; #2) -0.26 ± 0.03; and standard-deviations (SD) were: #1) 0.05 ± 0.04; #2) 0.09 ± 0.02. Without regularization, biases were #1) -0.09 ± 0.17; #2) -0.25 ± 0.20; SD values were: #1) 0.39 ± 0.04; #2) 0.38 ± 0.08.

Keywords*—*Quantitative ultrasound (QUS), Tissue characterization, Local attenuation estimation, Backscatter coefficient (BSC) estimation, LASSO, Regularization, Parametric maps.

I. INTRODUCTION

In quantitative ultrasound (QUS), constructing semantic parametric maps based on backscatter coefficient (BSC) modeling or local attenuation coefficient slope (ACS) remains a challenge. These maps may be useful for detecting lesions or anatomical objects, or for characterizing anomalies within organs. The objective of this work was to propose a methodology for constructing regularized parametric maps in the case of linear fitting models. The proposed method was tested on: *1*) the spectral Gaussian fit (SGF) BSC model [1, 2], comprising the acoustic concentration and effective scatterer size; and *2*) the spectral log-difference (SLD) model [1, 3, 4], yielding the local ACS.

Previous works include a framework for BSC estimation, based on the power law model for BSC [5], comprising a quadratic regularization term that is solved using dynamic programming [6]. A framework for local ACS estimation, based on the SLD method, and a total variation regularization term was proposed in [7] and was solved using the alternating direction method of multipliers (ADMMs) [8].

In this work, regularization was formulated as generalized LASSO [9], upon setting a locally constant trend constraint on regression coefficients, with variable Lagrangian multiplier (LM). Then, a novel strong Bayesian Information Criterion (BIC) [10] was applied for model selection of the LM, thus yielding regularized parametric maps.

II. THEORETICAL FRAMEWORK

A. Power spectrum modeling

Based on acoustical physics, the power spectrum of received radiofrequency signals at depth z (cm) can be modeled [1] as a function of frequency, denoted f (MHz), in the form of a product of 4 factors: *i*) a factor due to electronics (including the transfer function); *ii*) the diffraction factor, which depends on the transducer's geometry; *iii*) the backscatter coefficient $BSC(f,z)$, which depends on the scattering medium; and *iv*) the total attenuation factor $A(f,z)$.

An acquisition of a reference phantom using the same settings as the samples' acquisition yields, after simplifications, the power spectra ratio:

$$\frac{PS(f,z)}{PS_{ref}(f,z)} = \frac{BSC(f,z)}{BSC_{ref}(f,z)} \frac{A(f,z)}{A_{ref}(f,z)}. \quad (1)$$

1) Under the SGF model, applied to the samples, one postulates a Gaussian BSC that depends on acoustic concentration, through a normalizing constant C, on speed of sound c in the scattering medium, and on the effective scatterers' radius a_{eff}. We also consider an attenuation factor of the form $A(f,z) = \exp(-4\alpha_{att}zf)$, where α_{att} (Neper/cm/MHz) is the total ACS. Under these hypotheses, one obtains [1, 2]:

$$\log \frac{PS(f,z)}{PS_{ref}(f,z)} = -4\Delta\alpha_{att}zf - 0.827\frac{4\pi^2}{c^2}\left(\Delta a_{eff}{}^2\right)f^2 + \Delta\log C, \quad (2)$$

where $\Delta\alpha_{att}$ is the difference in ACS (Neper/cm/MHz) between samples and the reference phantom, Δa_{eff}^2 (m^2) is the corresponding difference in squared effective radii of scatterers, and $\Delta\log C$ (no units) is the corresponding difference in acoustic concentration in log-scale.

2) In the case of the SLD model, one considers two non-overlapping windows within a region of interest (ROI) at proximal and distal depths z_p and z_d, respectively. The attenuation factors at depths z_p and z_d are related as:

$$A(f, z_d) = A\left(f, z_p\right)\exp(-4\alpha_0\Delta z f), \quad (3)$$

where α_0 is the local ACS and $\Delta z = z_d - z_p$. Furthermore, one assumes that the BSCs at two depths are proportional, which under the Gaussian model means that the scatterers' radius remains fixed within the ROI, but that the acoustic concentration might vary. One then obtains the relation [1, 3, 4]:

$$\log\frac{PS_s(f,z_p)}{PS_s(f,z_d)} - \log\frac{PS_{ref}(f,z_p)}{PS_{ref}(f,z_d)} = 4\Delta\alpha_0\Delta z f + const, \quad (4)$$

where $\Delta\alpha_0$ is the difference in local ACS between the sample and the reference phantom.

B. *Data fidelity term*

In LASSO framework, the data fidelity term is the usual linear regression residual fit [9]:

$$\text{fit}(y,\beta) = \frac{1}{2}\sum_{r=1}^{N_{ROI}}\|y_r - X_r\beta_r\|_2^2 \quad (5)$$

where N_{ROI} is the number of ROIs for the estimation of parameters. For each ROI r, $y_r = \left(y_r(f_i)\right)_{i=1}^{N_{Freq}}$ represents the observed spectral data expressed at each frequency f_i (MHz) of the discretized usable frequency range. Moreover, the matrix X_r represents the model's predictors (based on the set of frequencies), while β_r represents regression coefficients (based on the considered model).

1) In the case of the SGF model, the observed spectral data $y_r(f_i)$ in the r-th ROI (at depth z_r) is the LHS of (2) evaluated at frequencies f_i. The predictors' matrix and vector of regression coefficients are then given by the RHS of (2), which yields:

$$\beta_r = \left(\Delta\alpha_{r,att} \quad 0.827\,4\pi^2/c^2\,\Delta a_{r,eff}^2 \quad \Delta\log C_r\right)^T. \quad (6)$$

2) In the case of the SLD model, the observed spectral data is the LHS of (4). The predictors' matrix and regression coefficients are obtained from the RHS of (4), which yields:

$$\beta_r = (\Delta\alpha_{r,0} \quad \beta_{r,2})^T. \quad (7)$$

C. *Regularization term*

In LASSO framework, the regularization term considered in this work is of the form [9]:

$$\text{reg}(\beta,\lambda) = \lambda\sum_{r=1}^{N_{ROI}}\sum_{k=1}^{d}\sum_{s\in N(r)}\left|\beta_{r,k} - \beta_{s,k}\right|, \quad (8)$$

where λ is the LM, which balances the weight of the constraint with respect to the data fidelity term, $d = 3$ for the SGF model and $d = 2$ for the SLD model, and $N(r)$ denotes the set of previous adjacent ROIs (along both axial and lateral directions) to a given ROI *r*. This regularizing term favors naturally identical regression coefficients between adjacent ROIs, and hence causes ROIs to get fused (*i.e.*, to share the same regression coefficients). For a given LM value λ, one seeks the vector of coefficients $\hat{\beta}(\lambda)$ that minimizes the corresponding energy functional $\text{fit}(y,\beta) + \text{reg}(\beta,\lambda)$.

D. *Model's selection*

The Bayesian Information Criterion (BIC) [10] yields in LASSO framework the expression:

$$BIC(\lambda) = N\log\left(\text{fit}\left(y,\hat{\beta}(\lambda)\right)\right) + \log N \times C(\lambda), \quad (9)$$

where $N = N_{ROI} \times N_{Freq}$ is the total sample size in the linear regression problem, and $C(\lambda)$ is the model's complexity, which is equal in this case to the number of regression coefficients (*i.e.*, the dimension d defined in Section II-C) times the number of distinct fused ROIs in $\hat{\beta}(\lambda)$.

Model's selection under the BIC is formulated as choosing the value of λ that minimizes the BIC curve [10]. To reach a greater number of fused ROIs, we propose a "strong BIC", which we define as selecting the maximal value of λ for which $BIC(\lambda) = BIC(0)$. Thus, the LM λ was maximized as to yield a BIC value no worse than that obtained without any constraint. The actual computation of the BIC curve was performed with our implementation of the path algorithm [9] using Matlab software (version R2018a, The MathWorks, Natick, MA).

III. METHODS

Phantoms were made with a mixture of agar (2%), glycerol (10%) and 4.5% or 12% of graphite powder (g.p.) [11]. Ground truth ACS values were estimated with a planar reflection method [12].

Acquisitions were performed with a Verasonics Vantage 256 (Redmond, WA) scanner using an ATL L7-4 probe (Philips, Bothell, WA) driven at 5 MHz. One hundred frames were obtained with 21 angles (-5º to 5º) compounding.

Radiofrequency data were f-k migrated [13] and averaged over all frames for noise removal. Power spectra were averaged over 15 scan lines, each spanning 10 pulse lengths, on overlapping ROIs. Acquisitions with same settings were made on a reference phantom (117GU-101 CIRS, Norfolk, VA).

IV. RESULTS

A. *Phantom's attenuation calibration*

Ground truth ACS values estimation yielded (in dB/cm/MHz) for the phantoms' two distinct media: #1) 0.56 ± 0.06 (4.5% g.p.); #2) 1.27 ± 0.09 (12% g.p.).

B. *Results*

1) Results for the SGF method: On phantoms with an inclusion (N = 4, #2 surrounded by #1), the contrast-to-noise ratio on difference in acoustic concentration (in log-scale) was 2.7 ± 0.22 (no units) with regularization, and 0.97 ± 0.13 without it. See Fig. 1 for examples of results.

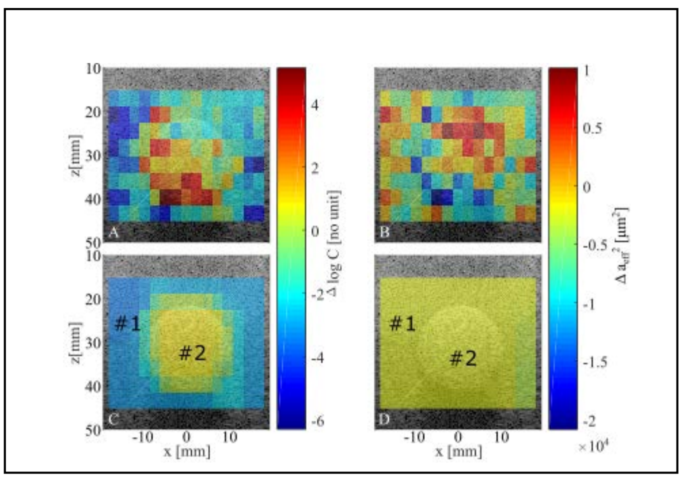

Fig. 1. Parametric maps based on the SGF method without (top panels A and B) and with the proposed regularization (bottom panels C and D). (Left) difference in acoustic concentration (log-scale) between an agar/graphite phantom and the CIRS reference phantom; (Right) difference in squared effective radii.

2) Results for the SLD method: On phantoms with side-by-side media (N = 3), biases were (dB/cm/MHz): #1) -0.11 ± 0.04; #2) -0.26 ± 0.03; and standard deviations (SD) were (dB/cm/MHz): #1) 0.05 ± 0.04; #2) 0.09 ± 0.02. Without regularization, biases were (dB/cm/MHz): #1) -0.09 ± 0.17; #2) -0.25 ± 0.20; SD values were (dB/cm/MHz): #1) 0.39 ± 0.04; #2) 0.38 ± 0.08. See Fig. 2 for examples of results.

V. DISCUSSION

The results indicate that the proposed regularization methodology does improve the contrast-to-noise ratio on difference in acoustic concentration (in log-scale) within the SGF framework. Moreover, the biases in local ACS, in the SLD framework, were similar with or without regularization, while SD values decreased substantially with regularization. Future works will include a comparison with previous regularization methods in QUS [6, 7].

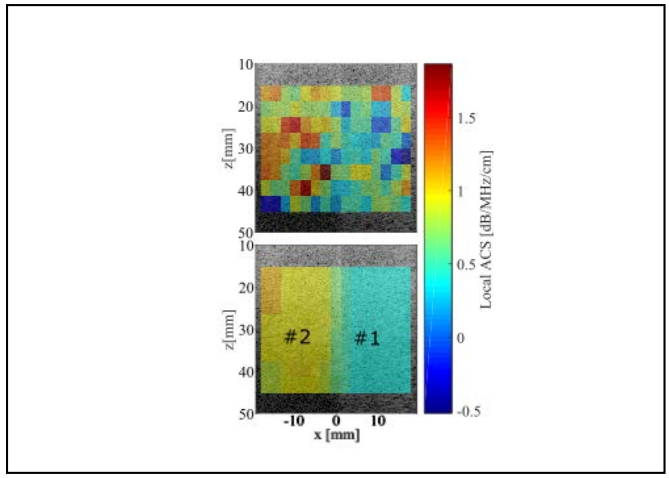

Fig. 2. Parametric maps of local ACS based on the SLD model without (top panel) and with the proposed regularization (bottom panel).

ACKNOWLEDGMENTS

This work was partially supported by an Audace grant number 2019-AUDC-263591 from the Fonds de Recherche du Québec, and by the Canadian Institutes of Health Research (grant #389385).

REFERENCES

[1] T. A. Bigelow and Y. Labyed, "Attenuation Compensation and Estimation," in Quantitative Ultrasound in Soft Tissues, J. Mamou and M. L. Oelze, Eds. New York: Springer, 2013, pp. 71-94.

[2] T. A. Bigelow and W. D. O'Brien, Jr., "Evaluation of the spectral fit algorithm as functions of frequency range and Δka_{eff}," *IEEE Trans. Ultrason., Ferroelect., Freq. Contr.*, vol. 52, pp. 2003-2010, November 2005.

[3] M. Insana, J. Zagzebski, E. Madsen, "Improvements in the spectral difference method for measuring ultrasonic attenuation," *Ultrasonic Imaging*, vol. 5, pp. 331-345, April 1983.

[4] Y. Labyed and T. A. Bigelow, "A theoretical comparison of attenuation measurement techniques from backscattered ultrasound echoes," *J. Acoust. Soc. Am.*, vol. 129, pp. 2316-2324, April 2011.

[5] K. Nam, J. A. Zagzebski, T. J. Hall, "Simultaneous backscatter and attenuation estimation using a least squares method with constraints," *Ultrasound Med. Biol.*, vol. 37, pp. 2096-2104, December 2011.

[6] Z. Vajihi, I. M. Rosado-Mendez, T. J. Hall, H. Rivaz, "Low variance estimation of backscatter quantitative ultrasound parameters using dynamic programming," *IEEE Trans. Ultrason., Ferroelect., Freq. Contr.*, vol. 65, pp. 2042-2053, November 2018.

[7] A. L. Caila and R. Lavarello, “Regularized spectral log difference technique for ultrasonic attenuation imaging,” *IEEE Trans. Ultrason., Ferroelect., Freq. Contr*., vol. 65, pp. 378-389, March 2018.

[8] P. Rodriguez and B. Wohlberg, “Efficient minimization method for a generalized total variation functional,” *IEEE Trans. Image Proc*., vol. 18, pp. 322-332, February 2009.

[9] R. J. Tibshirani and J. Taylor, “The solution path of the generalized lasso,” *Ann. Stat.*, vol. 39, pp. 1335-1371, March 2011.

[10] G. Schwartz, “Estimating the dimension of a model,” *Ann. Stat*., vol. 6, pp. 461-464, February 1978.

[11] E. L. Madsen, J. A. Zagzebski, R. A. Banjavie, R. E. Jutila, “Tissue mimicking materials for ultrasound phantoms,” *Med. Phys*., vol. 5, pp. 391-393, May 1978.

[12] K. A. Wear, T. A. Stiles, G. R. Frank, E. L. Madsen, F. Cheng, E. J. Feleppa, C. S. Hall, B. S. Kim, P. Lee, W. D. O’Brien, Jr, M. L. Oelze, B. I. Raju, K. K. Shung, T. A. Wilson, J. R. Yuan, “Interlaboratory comparison of ultrasonic backscatter coefficient measurements from 2 to 9 MHz,” *J. Ultrasound Med*., vol. 24, pp. 1235-1250, September 2005.

[13] D. Garcia, L. Le Tarnec, S. Muth, E. Montagnon, J. Porée, G. Cloutier, “Stolt’s f-k migration for plane wave ultrasound imaging,” *IEEE Trans. Ultrason., Ferroelect., Freq. Contr.*, vol. 60, pp. 1853-1867, September 2013.